CONFIDENTIAL

NACA RM L53G14

NACA

RESEARCH MEMORANDUM

WING LOADS ON THE BELL X-1 RESEARCH AIRPLANE (10-PERCENT-THICK WING) AS DETERMINED BY PRESSURE-DISTRIBUTION MEASUREMENTS IN FLIGHT AT SUBSONIC AND TRANSONIC SPEEDS

By Ronald J. Knapp and Gareth H. Jordan

Langley Aeronautical Laboratory
Langley Field, Va.

NATIONAL ADVISORY COMMITTEE
FOR AERONAUTICS

WASHINGTON

November 4, 1953

CONFIDENTIAL

NATIONAL ADVISORY COMMITTEE FOR AERONAUTICS

RESEARCH MEMORANDUM

WING LOADS ON THE BELL X-1 RESEARCH AIRPLANE (10-PERCENT-THICK WING) AS DETERMINED BY PRESSURE-DISTRIBUTION MEASUREMENTS IN FLIGHT AT SUBSONIC AND TRANSONIC SPEEDS

By Ronald J. Knapp and Gareth H. Jordan

SUMMARY

Measurements of wing loads have been made on the left wing of the Bell X-1 (10-percent-thick wing) research airplane. Data are presented within a wing-panel normal-force coefficient range from -0.2 to 1.0 at Mach numbers from about 0.50 to 1.19.

The results of the investigation indicated that the wing-panel span loading was approximately elliptical at values of wing-panel normal-force coefficient from 0.3 up to the limit of the tests for subcritical and slightly supercritical Mach numbers (M = 0.56 and 0.75) and for higher transonic Mach numbers (M = 0.97 and 1.17). At Mach numbers from 0.83 to between 0.88 and 0.97 there was a deviation from this elliptical type loading, which may be attributed chiefly to shock formation and movement with changes in Mach number.

The spanwise center of pressure for the wing-panel load, at values of wing-panel normal-force coefficient from 0.3 to 0.6, was located at 52 to 53 percent wing semispan for Mach numbers from 0.50 to about 0.73 and from 0.96 to 1.17. A slight outboard shift of about 2 percent wing semispan occurred at Mach numbers from about 0.73 to 0.96. There were pronounced Mach number and normal-force effects on the chordwise center-of-pressure location in the Mach number range where shock movement on both the upper and lower surfaces of the wing was rapid ($M \approx 0.73$ to 0.96). At subcritical Mach numbers the center of pressure was located at about 25 percent wing mean aerodynamic chord and at Mach numbers above 0.96 was located at about 41 percent wing mean aerodynamic chord.

Theoretical methods used for determining span loading gave a good approximation of the flight data except in the region where shock formation and movement occurred and caused the loading to deviate from the elliptical type. These methods adequately predicted the coefficient of

bending moment throughout the Mach number range tested, including the Mach number range where these methods did not closely predict the shape of the span loading.

The normal-load parameter dropped rapidly from the wing-panel root to the airplane center line. In general, the loading parameter at the airplane center line was about half of that at the wing-panel root station.

INTRODUCTION

The NACA High-Speed Flight Research Station at Edwards Air Force Base, Calif. has conducted a series of flight tests on the Bell X-1 research airplane in the subsonic and transonic speed range for the measurement of wing and fuselage loads. The purpose of this paper is to present an analysis of the wing loads as obtained on the left wing of the airplane by pressure-distribution measurements at six spanwise stations. The data were obtained for Mach numbers from about 0.30 to 1.19 at altitudes from 17,000 to 47,000 feet in level flight, low-speed stalls, push-overs, and in pull-ups to high lift. Most of these data have been presented previously in unanalyzed tabular form in references 1 to 4. An analysis of the pressure distributions obtained at four of the individual spanwise stations (stations A, C, D, and F) is given in reference 5. Some additional section pressure-distribution data at station D have been presented in reference 6. A comparison of some of the flight data of references 1 to 4 with data obtained in the Langley 16-foot transonic tunnel on a quarter-scale model of the airplane is given in reference 7.

In order that some wing-to-fuselage carry-over data might be obtained, tests were made in which fuselage pressures were measured near the wing and results are included herein.

SYMBOLS

b wing span (28 ft)

C_{b_P} wing-panel bending-moment coefficient about center line of airplane, $\int_{0.184}^{1} c_n \frac{c}{\bar{c}} \frac{2y}{b} d\frac{2y}{b}$

$\left(C_{m_{c'/4}}\right)_P$ wing-panel pitching-moment coefficient about wing 0.25 mean aerodynamic chord, $\frac{\bar{c}}{c'}\int_{0.184}^{1} c_m\left(\frac{c}{\bar{c}}\right)^2 d\,\frac{2y}{b}$

C_N wing normal-force coefficient, including carry over to fuselage, $\int_0^1 c_n \frac{c}{\bar{c}}\, d\,\frac{2y}{b}$

C_{N_P} wing-panel normal-force coefficient, $\int_{0.184}^{1} c_n \frac{c}{\bar{c}}\, d\,\frac{2y}{b}$

C_{N_A} airplane normal-force coefficient, nW/qS

c local wing chord parallel to plane of symmetry, ft

$\bar{c}$ average chord of wing (4.64 ft), S/b

c' wing mean aerodynamic chord (4.80 ft), $\bar{c}\int_0^1 \left(\frac{c}{\bar{c}}\right)^2 d\,\frac{2y}{b}$

c_m section pitching-moment coefficient about a line perpendicular to longitudinal axis of airplane, passing through 0.25-chord point of wing mean aerodynamic chord, $\int_0^1 -P_R\left(\frac{x}{c} - \frac{0.40c - 0.15c'}{c}\right) d\,\frac{x}{c}$

c_n section normal-force coefficient, $\int_0^1 P_R\, d\,\frac{x}{c}$

M free-stream Mach number

n normal-load factor

P_R resultant pressure coefficient,

$$\frac{\text{lower-surface pressure - upper-surface pressure}}{q}$$

q free-stream dynamic pressure, lb/sq ft

S wing area, including area projected through fuselage (130 sq ft)

W	airplane weight, lb
x	chordwise distance from section leading edge, ft
y	spanwise distance outboard of airplane center line, ft
α	airplane angle of attack, deg

Subscript:

max	maximum

DESCRIPTION OF AIRPLANE WING

The Bell X-1 research airplane used in these tests and the general over-all dimensions are shown in the photograph and three-view drawing presented as figures 1 and 2, respectively.

The airplane had a wing of aspect ratio 6, taper ratio of 0.5, and had an incidence angle with respect to the fuselage axis of 2.5° at the airplane center line and 1.5° at the wing tip. A line through the 40 percent local chords was perpendicular to the plane of symmetry and the wing had a modified NACA 65-110 airfoil section. Over the flap stations (stations A to C; see fig. 3) the airfoil was modified rearward of the 85-percent-chord point to give a finite thickness at the trailing edge. For the aileron stations (stations D to F) the cusp was replaced by a straight taper rearward of the 85-percent-chord point to reduce hinge moments (ref. 8). The ordinates of the modified airfoil sections are presented in table I.

The fuselage, which is a body of revolution having a fineness ratio of 6.8 with its maximum diameter in the vicinity of the wing leading edge, enclosed approximately 19 percent of the wing area. Pressures were measured on the fuselage surface area between the leading and trailing edges of the wing.

The locations of the pressure-measuring orifices are shown in figure 3. The wing and fuselage was painted and polished during the tests, but no refined filling or smoothing was attempted.

INSTRUMENTATION AND DATA REDUCTION

Standard NACA instrumentation was used to measure all surface pressures (using two 60-cell recording flight manometers), normal acceleration,

rolling velocity, and control position. Indicated free-stream static and dynamic pressures were measured with a pitot-static tube ahead of the fuselage nose. All records were synchronized by a common timer. Mach number and free-stream static pressure were obtained from the indicated free-stream static and dynamic pressures by the radar tracking method of reference 9. All surface pressures were measured relative to the pressure in the instrument compartment. The instrument compartment pressure was measured relative to the indicated free-stream static pressure, which was corrected to the true free-stream static pressure as described.

Wing and fuselage surface pressures were obtained from 1/8-inch-diameter flush-type orifices installed in the surfaces. The orifices were connected to the instrument compartment by 1/8-inch inside-diameter aluminum tubing. The length of aluminum tubing varied from about 14 feet at the tip to about 2 feet at the wing-panel root and fuselage. Approximately 3 feet of 3/16-inch inside-diameter rubber tubing was used to connect each aluminum tube to the manometer cell. The effects of lag in the measurement of surface pressures have been neglected inasmuch as these effects have been found to be insignificant at the rates at which the pressures were changing during these tests.

The section resultant-pressure-distribution plots were mechanically integrated to obtain values of section normal-force and pitching-moment coefficient, which were used to construct spanwise load- and moment-distribution plots. These spanwise plots were obtained for flight conditions throughout the maneuvers. From these plots the representative spanwise load plots presented in this paper were selected. The entire group of spanwise load- and moment-distribution plots were mechanically integrated to obtain normal-force coefficient, pitching-moment coefficient, and bending-moment coefficient. From these values spanwise and chordwise wing centers of pressure were obtained. The data presented are in the form of cross plots of the data in order that normal-force coefficient or Mach number might be held constant. All wing-panel coefficients have been based on the entire wing area, whereas they were based only on wing-panel area in references 1 to 4 and reference 7. This change has been made in order to facilitate presentation of the load carry over to the fuselage.

Fuselage pressure data were obtained in the vicinity of the wing in additional tests to get an indication of wing-to-fuselage load carry over. These data were matched with the wing data on the basis of similar Mach number and airplane normal-force flight conditions in order to obtain complete spanwise load plots.

TESTS

The data presented herein were obtained during unaccelerated stalls at Mach numbers less than 0.50, during pull-ups and push-overs (at approximately constant M) at Mach numbers from 0.53 to 1.19, and during level flight from a Mach number of 0.79 to 1.00. The low-speed data were obtained at altitudes down to about 17,000 feet and the high-speed data were obtained at higher altitudes, up to about 47,000 feet. During all the maneuvers from which data are presented the rolling velocities were low and the ailerons were held close to neutral ($\pm 1^{\circ}$). Tabulated data have been presented in references 1 to 4 throughout many of the specific maneuvers covered in this paper.

ACCURACY

The accuracy of the test results is estimated to be within the following limits:

M	± 0.01
P_R	± 0.03
C_{N_P}	± 0.05
$\left(C_{m_{c'}}/4\right)_P$	± 0.006
C_{b_P}	± 0.03

RESULTS AND DISCUSSION

Span Load Distributions

The variation across the span of the chordwise load distributions for a C_{N_P} of approximately 0.3 at Mach numbers from 0.56 to 1.19 is shown as isometric views in figure 4. The effect of Mach number on the spanwise loading is shown by figure 5 for the same conditions as shown in the isometric views. It may be seen from figure 5 that for subcritical and slightly supercritical Mach numbers (M = 0.56 and 0.75) and for higher transonic Mach numbers (M = 0.97 and 1.19) the span loading at a C_{N_P} of 0.3 was approximately elliptical. At lower transonic Mach numbers (M = 0.83 to between 0.88 and 0.97) there was a deviation from this elliptical-type loading, which may be attributed chiefly to formation and movement of the shocks with changes in Mach number. Some of the effects of shock formation and movement on chordwise loading can be seen

in figure 4, where the most obvious effect is the relatively large region of down load near the midsemispan at a Mach number of 0.88. A detailed analysis of the chordwise pressure distributions and section characteristics throughout the normal-force and Mach number range may be found in reference 5.

The span loadings throughout the normal-force range of the tests are shown in figure 6 for selected Mach numbers from 0.56 to approximately 1.17. The approximate fraction of the total airplane normal force carried by the wing panels outboard of station A (18.4 percent wing semispan) is shown in figure 7 for C_{N_A} values from 0.3 to 0.7 throughout the Mach number range. The portion of the airplane load carried by the wing panels varied from about 70 to 85 percent because of the change in angle of attack with Mach number necessary to maintain any given C_{N_A} in this range and because of the change with Mach number of balancing tail load. In order that an indication of the airplane angle of attack might be had for any normal-force coefficient and Mach number of the tests, figure 8 is presented. The data of this figure were obtained from additional flights.

Basic loading.- The basic loading $\left(C_{N_P} = 0\right)$ across the span for Mach numbers of 0.56, 0.82, and 0.97 may be seen in figure 6. Experimental data were not available at $C_{N_P} = 0$ for the other Mach numbers covered in figure 6.

The basic span loading shows a negative loading to about 50 percent wing semispan with positive loading outboard of that station throughout the Mach number range tested. The inboard stations are at a higher angle of attack than the outboard stations due to the 1° of wing twist. For a wing alone this would normally be expected to cause the reverse of the type of loading found. The combination of positive wing incidence and camber, however, gave the fuselage a negative angle of attack for $C_{N_P} = 0$. At this negative angle of attack the fuselage produced negative lift which affected the inboard stations.

Total (basic plus additional) loading.- The span loadings throughout the normal-force range of the tests are shown in figure 6 for Mach numbers from 0.56 to approximately 1.17.

For low values of normal-force coefficient $\left(C_{N_P} \leq 0.2\right)$ it may be seen that the span-load distributions deviate slightly from elliptical loading and, at Mach numbers from 0.56 through 0.82, showed the same loss over the inboard portion as did the basic loading. The negative angle of attack of the fuselage, as explained for the basic loading, is thought to be the chief cause of this deviation, as it is estimated that the fuselage does not reach a zero angle of attack at values of C_{N_P}

below about 0.2. At a Mach number of 0.97 (the highest Mach number for which data are available at values of C_{N_P} less than 0.3) the loss of lift over the inboard stations, due to fuselage interference, is diminished. In reference 5 it was shown that at this Mach number supersonic flow existed over the entire wing-panel root chord. The shape of the wing-fuselage juncture would tend to give a supersonic expansion and thus decrease the loss of lift over the inboard stations at this Mach number.

At the higher normal-force coefficients (C_{N_P} = 0.3 to the limit of the tests), the span-load distributions varied with Mach number and at some Mach numbers with normal-force coefficient. At subcritical speeds the section load distributions were similar in shape across the span, but of decreasing magnitude as the tip was approached because of wing taper and the relieving effects of the tip. These effects caused the typical elliptical subsonic loading seen at M = 0.56 which existed to the highest C_{N_P} reached. At Mach numbers near 0.75, it was shown in reference 5 that the critical speed has been surpassed over most of the span, but that the variation in shape of the section pressure distributions across the span is not appreciable. Hence, the nearly elliptical loading is maintained to this Mach number.

Large deviations from the elliptical spanwise load distributions occurred at Mach numbers of 0.82 and 0.88 (fig. 6) at values of C_{N_P} from 0.3 to the maximum value tested. As is pointed out in reference 5, there is a region of reduced chordwise loading in this Mach number region, rearward of the upper surface shock and forward of the lower surface shock. There is, however, a spanwise variation in the extent and magnitude of this reduced loading; the variation being particularly apparent at wing station D where it is greatest and at the root and tip stations where the reduced loading is least. This spanwise variation is most obvious at M = 0.88, where it causes a large dip in the span loading curve at 64.5 percent wing semispan and the higher root and tip values.

At Mach numbers of 0.97 and 1.17 the spanwise loadings are again nearly elliptical throughout the C_{N_P} range tested. This elliptical spanwise loading may be attributed to the fact that, as shown in reference 5, the flow over the entire chord is supersonic and the shocks are located at the trailing edge; a condition resulting in similar chordwise load distributions across the span.

Comparison of theory with flight test.- A comparison of empirically and theoretically determined span loadings (refs. 10 and 11) with flight data has been made at Mach numbers of 0.56, 0.82, 0.97, and 1.17 and is given by figure 6. For the theory and empirical calculations an isolated

wing of aspect ratio 6 was assumed and no fuselage effect was considered. The portion of the loading outboard of station A (18.4 percent semispan) has been shown for several values of C_{N_P}. The span loadings predicted by the empirical method (ref. 10) and theory (ref. 11) are in close agreement with each other.

For the basic and low lift conditions the theoretical methods show a more positive inboard and less positive outboard loading than does the experimental method. This difference may be attributed to the fact that the lift over the inboard wing stations was affected by the fuselage which was at a negative angle of attack in this lift range and was not accounted for.

At the higher values of C_{N_P} the theoretical methods show span loadings that are approximately elliptical at Mach numbers of 0.56, 0.82, and 0.94. The empirical method of reference 10 was calculated for a Mach number of 0.94 (approximate limit for which it may be calculated) for the purpose of comparison with the flight data at a Mach number of 0.97. These empirical span loadings at $M = 0.94$ have been compared also with the flight data at $M = 1.17$ because of the similarity of the flight data at $M = 1.17$ with the data at $M = 0.97$. The theoretical methods gave a good approximation of the experimentally determined spanwise loading at Mach numbers of 0.56, 0.97, and 1.17. At a Mach number of 0.82, however, the agreement of the shape of the theoretical span loading with the experiment was poor because of the inability of the theoretical methods to account for shock effects, which were the causes of the nonelliptical-type loading encountered at Mach numbers of 0.82 and 0.88 (fig. 6).

Wing-Panel Aerodynamic Characteristics

Spanwise center of pressure and bending-moment coefficient.- The variation of spanwise center of pressure and bending-moment coefficient with Mach number for values of C_{N_P} of 0.3 to 0.6 is shown in figure 9. The bending-moment coefficient increased linearly with an increase in C_{N_P} $\left(C_{N_P} = 0.3 \text{ to } 0.6\right)$ throughout the Mach number range investigated. At Mach numbers from 0.50 to about 0.73 and between 0.96 and 1.17 the spanwise center of pressure was located at 52 to 53 percent semispan; consequently, the bending-moment coefficient showed no variation with Mach number in this range. At Mach numbers from about 0.73 to 0.96 a slight outboard shift of about 2 percent semispan occurred in the center-of-pressure location with a corresponding small increase in the bending-moment coefficient. The outboard shift in center-of-pressure location was caused by the down load near the midsemispan resulting in an increase in the load carried by the tip stations.

The theoretical and empirical methods of references 10 and 11, discussed in the previous section, adequately predicted the coefficient of bending-moment (fig. 9) for this configuration throughout the Mach number range tested, including the Mach number range where these methods did not closely predict the shape of the span loading.

Chordwise center of pressure and pitching-moment coefficient.- The variation of chordwise center of pressure of the wing panel for values of C_{N_P} from 0.2 to 0.6 (fig. 10) shows large changes with Mach number similar to the section data of reference 5.

At the subcritical and slightly supercritical Mach numbers of the tests ($M = 0.50$ to about 0.73), the center of pressure was located at 23 to 26 percent wing mean aerodynamic chord for all values of C_{N_P} presented and showed no variation with Mach number. This nonvarying position of the center of pressure was due to the fact that the chordwise loadings at each of the spanwise stations showed little deviation from the typical subsonic loading throughout this Mach number range (ref. 5).

No appreciable change in center-of-pressure location occurred with C_{N_P} or Mach number in the Mach number region in which supersonic flow existed over the entire wing ($M \approx 0.96$ to 1.17). In this range the chordwise center of pressure was located at approximately 41 percent wing mean aerodynamic chord.

In the Mach number range where shock movement on both the upper and lower surfaces of the wing is rapid ($M \approx 0.73$ to 0.96), however, there were pronounced Mach number and normal-force effects upon the center-of-pressure location. At a value of C_{N_P} of 0.2 the center of pressure moved rearward rapidly with increasing Mach number, reaching a location of about 39 percent of the wing mean aerodynamic chord at $M = 0.83$, above which an abrupt forward movement occurred (reaching about 16 percent at $M = 0.89$). With a further increase in Mach number from 0.89 to about 0.96 the center of pressure again moved rapidly rearward to the vicinity of the 40 percent wing mean aerodynamic chord. At the higher values of C_{N_P} similar trends in the movement of chordwise center of pressure with Mach number are seen but are less abrupt.

The variation with Mach number of pitching-moment coefficient for the wing panel, from which chordwise center of pressure was obtained, is also shown in figure 10 for values of C_{N_P} throughout the range tested. As in the case of chordwise center of pressure, there was very little change in pitching-moment coefficient with Mach number in the ranges from $M = 0.50$ to 0.73 and $M = 0.96$ to 1.17. There were large

changes in pitching-moment coefficient in the Mach number range from 0.73 to 0.96 accompanying the large center-of-pressure movement in this range.

The variation of pitching-moment coefficient with normal-force coefficient for various Mach numbers is shown in figure 11. At Mach numbers of 0.60 and 0.75 the wing is slightly unstable up to a moderately high normal-force coefficient $\left(C_{N_P} = 0.5\right)$ with an increase in stability as C_{N_P} was increased to 0.6. At a Mach number of 0.84 the wing is neutrally stable at C_{N_P} values from 0.2 to 0.3 with an increase in stability as C_{N_P} was increased to 0.6. In the Mach number range from 0.88 to 1.17 a definitely stable variation of pitching-moment coefficient with normal-force coefficient occurred at all values of normal-force coefficient tested.

Wing-to-Fuselage Carry Over

Fuselage resultant pressure distributions were obtained at three spanwise stations on the fuselage surface between the leading and trailing edges of the enclosed wing in order that some information as to the extent of the wing load carry over to fuselage might be obtained. The data were obtained at four selected airplane Mach numbers and are presented for comparison with wing station A at airplane normal-force coefficients of 0.35, 0.50, and 0.70 in figure 12.

The resultant pressure distributions show that, in general, the chordwise loading on the fuselage stations was decreased as the airplane center line was approached from wing station A. The peak loading near the leading edge of the wing was not apparent on any of the fuselage stations.

The chordwise loading at the fuselage station nearest the wing (row 3), as expected, showed the closest similarity to that at wing station A at all values of Mach number and C_{N_A} tested. The shock location on the upper surface of row 3 for $C_{N_A} = 0.35$ may be seen in figure 12 to be about the same as that at station A at a Mach number of 0.79, and to be about 15 percent chord behind it at Mach numbers of 0.84 and 0.88. At the higher values of C_{N_A} presented these shocks (station A and row 3) are seen to be closer in agreement than at $C_{N_A} = 0.35$ for $M = 0.84$ and 0.88. In general, the upper surface shock at these Mach numbers became poorly defined at fuselage rows 1 and 2 but appeared to move rearward, accompanied by a reduction in strength as the airplane center line was approached. At Mach numbers around 1.0 the shock had

reached the trailing edge at all fuselage rows, leaving an approximately rectangular load distribution. Additional pressures measured on the fuselage indicated that a major portion of the load carried by these fuselage stations was due to the carry over from the wing pressures.

The effect of Mach number on spanwise load distribution, including the load over the fuselage stations, is shown in figure 13 for C_N values of 0.30, 0.45, and 0.70. In order that these span loadings may be correlated with the loadings of figures 5, 6, and 12, tabulated values of C_{N_P} and C_{N_A} are included. The figure shows that the normal-load parameter dropped rapidly from the wing-panel root to the airplane center line. In general, the loading parameter at the airplane center line was about half of that at wing station A. In the Mach number region near 0.88 the airplane angle of attack necessary to attain a given C_N was greatest, because of the region of decreased wing-panel loading rearward of the upper-surface shock discussed in reference 5. Because of this increased angle of attack the fuselage stations contributed a relatively greater portion of the span load.

CONCLUSIONS

Results of measurements of wing loads over the wing of the Bell X-1 research airplane indicate that:

1. The wing-panel span loading was approximately elliptical at values of wing-panel normal-force coefficient from 0.3 up to the limit of the tests for subcritical and slightly supercritical Mach numbers (M = 0.56 and 0.75) and for higher transonic Mach numbers (M = 0.97 and 1.17). At Mach numbers from 0.83 to between 0.88 and 0.97 there was a deviation from this elliptical-type loading, which may be attributed chiefly to shock formation and movement with changes in Mach number.

2. The spanwise center of pressure for the wing-panel load, at values of wing-panel normal-force coefficient from 0.3 to 0.6, was located at 52 to 53 percent wing semispan for Mach numbers from 0.50 to about 0.73 and between 0.96 and 1.17. A slight outboard shift of about 2 percent wing semispan occurred at Mach numbers from about 0.73 to 0.96.

3. There were pronounced Mach number and normal-force effects on the chordwise center-of-pressure location in the Mach number range where shock movement on both the upper and lower surfaces of the wing was rapid ($M \approx 0.73$ to 0.96). At subcritical Mach numbers the center of pressure was located at about 25 percent wing mean aerodynamic chord and at Mach numbers above 0.96 was located at about 41 percent wing mean aerodynamic chord.

4. Theoretical methods used for determining span loading gave a good approximation of the flight data except in the region where shock formation and movement on the wing occurred and caused the loading to deviate from the elliptical shape. These methods adequately predicted the coefficient of bending moment throughout the Mach number range tested, including the Mach number range where these methods did not closely predict the shape of the span loading.

5. The normal-load parameter dropped rapidly from the wing-panel root to the airplane center line. In general, the loading parameter at the airplane center line was about half of that at the wing-panel root station.

Langley Aeronautical Laboratory,
National Advisory Committee for Aeronautics,
Langley Field, Va., June 26, 1953.

REFERENCES

1. Carner, H. Arthur, and Payne, Mary M.: Tabulated Pressure Coefficients and Aerodynamic Characteristics Measured on the Wing of the Bell X-1 Airplane in Level Flight at Mach Numbers From 0.79 to 1.00 and in a Pull-Up at a Mach Number of 0.96. NACA RM L50H25, 1950.

2. Knapp, Ronald J., and Wilken, Gertrude V.: Tabulated Pressure Coefficients and Aerodynamic Characteristics Measured on the Wing of the Bell X-1 Airplane in Pull-Ups at Mach Numbers From 0.53 to 0.99. NACA RM L50H28, 1950.

3. Smith, Lawrence A.: Tabulated Pressure Coefficients and Aerodynamic Characteristics Measured on the Wing of the Bell X-1 Airplane in an Unaccelerated Stall and in Pull-Ups at Mach Numbers of 0.74, 0.75, 0.94, and 0.97. NACA RM L51B23, 1951.

4. Knapp, Ronald J.: Tabulated Pressure Coefficients and Aerodynamic Characteristics Measured on the Wing of the Bell X-1 Airplane in an Unaccelerated Low-Speed Stall, in Push-Overs at Mach Numbers of 0.83 and 0.99, and in a Pull-Up at a Mach Number of 1.16. NACA RM L51F25, 1951.

5. Knapp, Ronald J., and Jordan, Gareth H.: Flight-Determined Pressure Distributions Over the Wing of the Bell X-1 Research Airplane (10-Percent-Thick Wing) at Subsonic and Transonic Speeds. NACA RM L53D20, 1953.

6. Carner, H. Arthur, and Knapp, Ronald J.: Flight Measurements of the Pressure Distribution on the Wing of the X-1 Airplane (10-Percent-Thick Wing) Over a Chordwise Station Near the Midspan, in Level Flight at Mach Numbers From 0.79 to 1.00, and in a Pull-Up at a Mach Number of 0.96. NACA RM L50H04, 1950.

7. Runckel, Jack F., and Henderson, James H.: A Correlation With Flight Tests of Results Obtained From the Measurement of Wing Pressure Distributions on a 1/4-Scale Model of the X-1 Airplane (10-Percent-Thick Wing). NACA RM L52E29, 1952.

8. Ormsby, C. A.: Aerodynamic Design of the MX-653 Wing. Rep. No. 44-943-008, Bell Aircraft Corp., June 5, 1945.

9. Zalovcik, John A.: A Radar Method of Calibrating Airspeed Installations on Airplanes in Maneuvers at High Altitudes and at Transonic and Supersonic Speeds. NACA Rep. 985, 1950. (Supersedes NACA TN 1979.)

10. Diederich, Franklin W.: A Simple Approximate Method for Calculating Spanwise Lift Distributions and Aerodynamic Influence Coefficients at Subsonic Speeds. NACA TN 2751, 1952.

11. DeYoung, John, and Harper, Charles W.: Theoretical Symmetric Span Loading at Subsonic Speeds for Wings Having Arbitrary Plan Form. NACA Rep. 921, 1948.

TABLE I.- AIRFOIL PROFILE AND ORDINATES OF THE BELL X-1 WING

[Abscissas and ordinates in percent of local chord]

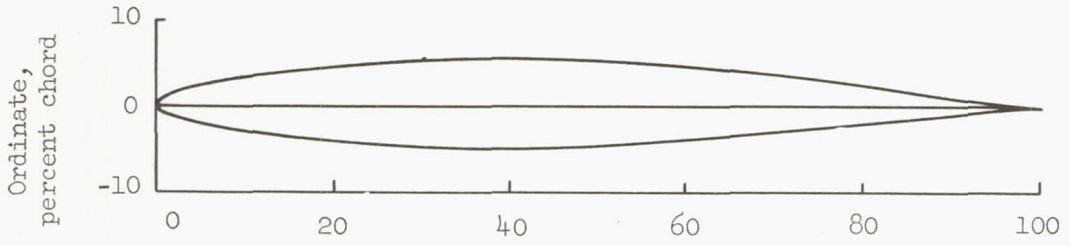

Modified NACA 65-110 airfoil section					
Upper surface			Lower surface		
Abscissa	Ordinate		Abscissa	Ordinate	
	Flap stations	Aileron stations		Flap stations	Aileron stations
0	0	0	0	0	0
.468	.796	.796	.533	-.746	-.746
.714	.966	.966	.786	-.896	-.896
1.210	1.222	1.222	1.290	-1.115	-1.115
2.454	1.667	1.667	2.546	-1.481	-1.481
4.949	2.334	2.334	5.051	-2.018	-2.018
7.447	2.859	2.859	7.553	-2.435	-2.435
9.947	3.298	3.298	10.053	-2.781	-2.781
14.949	4.002	4.002	15.051	-3.329	-3.329
19.954	4.541	4.541	20.046	-3.745	-3.745
24.961	4.951	4.951	25.039	-4.056	-4.056
29.968	5.246	5.246	30.032	-4.274	-4.274
34.976	5.439	5.439	35.024	-4.409	-4.409
39.984	5.532	5.532	40.016	-4.461	-4.461
44.992	5.511	5.511	45.008	-4.416	-4.416
50.000	5.364	5.364	50.000	-4.261	-4.261
55.007	5.078	5.078	54.993	-3.983	-3.983
60.013	4.682	4.682	59.987	-3.611	-3.611
65.018	4.197	4.197	64.982	-3.167	-3.167
70.021	3.642	3.642	69.979	-2.670	-2.670
75.023	3.032	3.032	74.977	-2.137	-2.137
80.022	2.385	2.385	79.978	-1.589	-1.589
85.019	1.721	1.721	84.981	-1.048	-1.048
90.000	1.100	1.148	90.000	-.687	-.698
95.000	.525	.574	95.000	-.295	-.349
100.000	.010	0	100.000	-.010	0
L. E. radius: 0.687 percent chord					

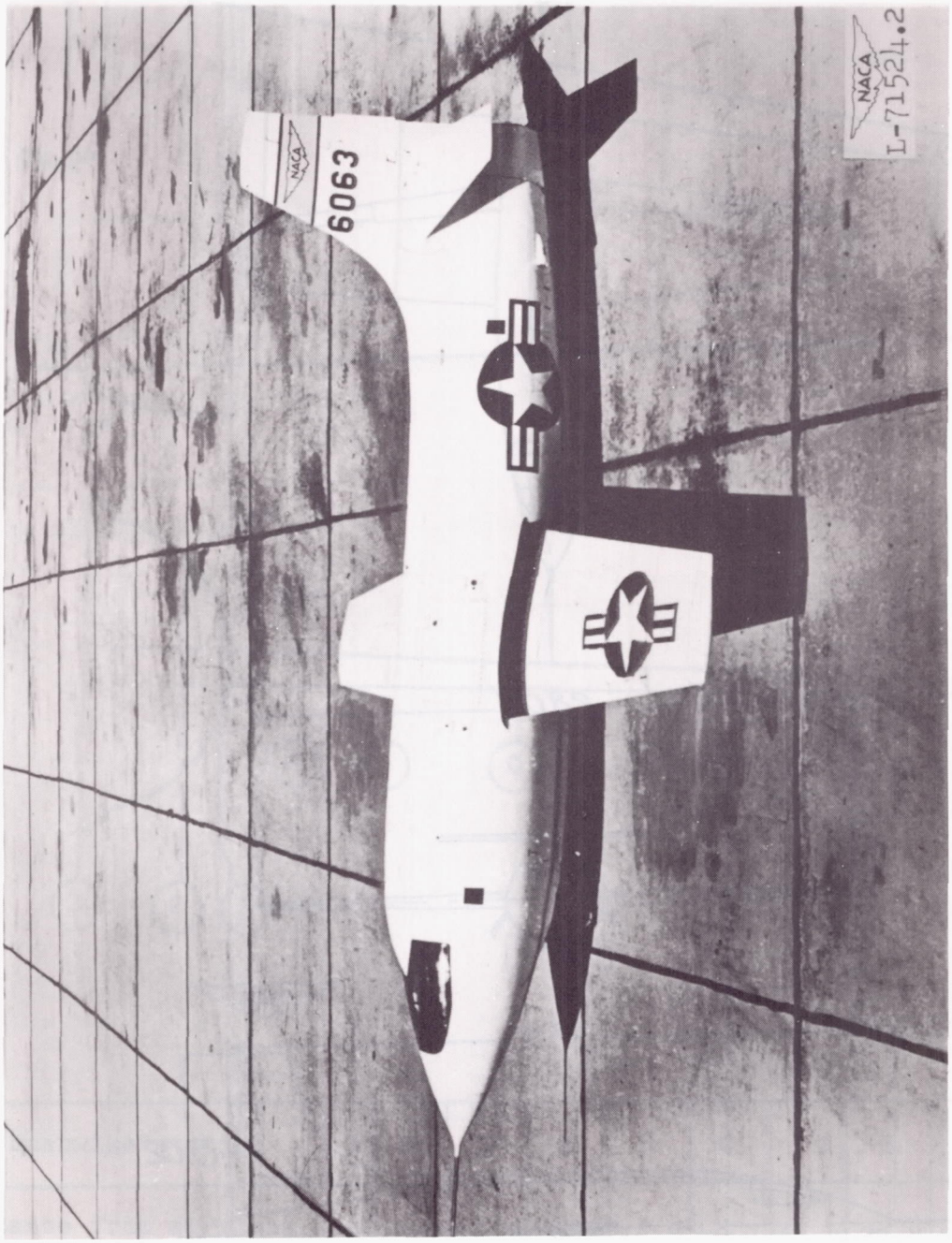

Figure 1.- Overhead side view of Bell X-1 airplane.

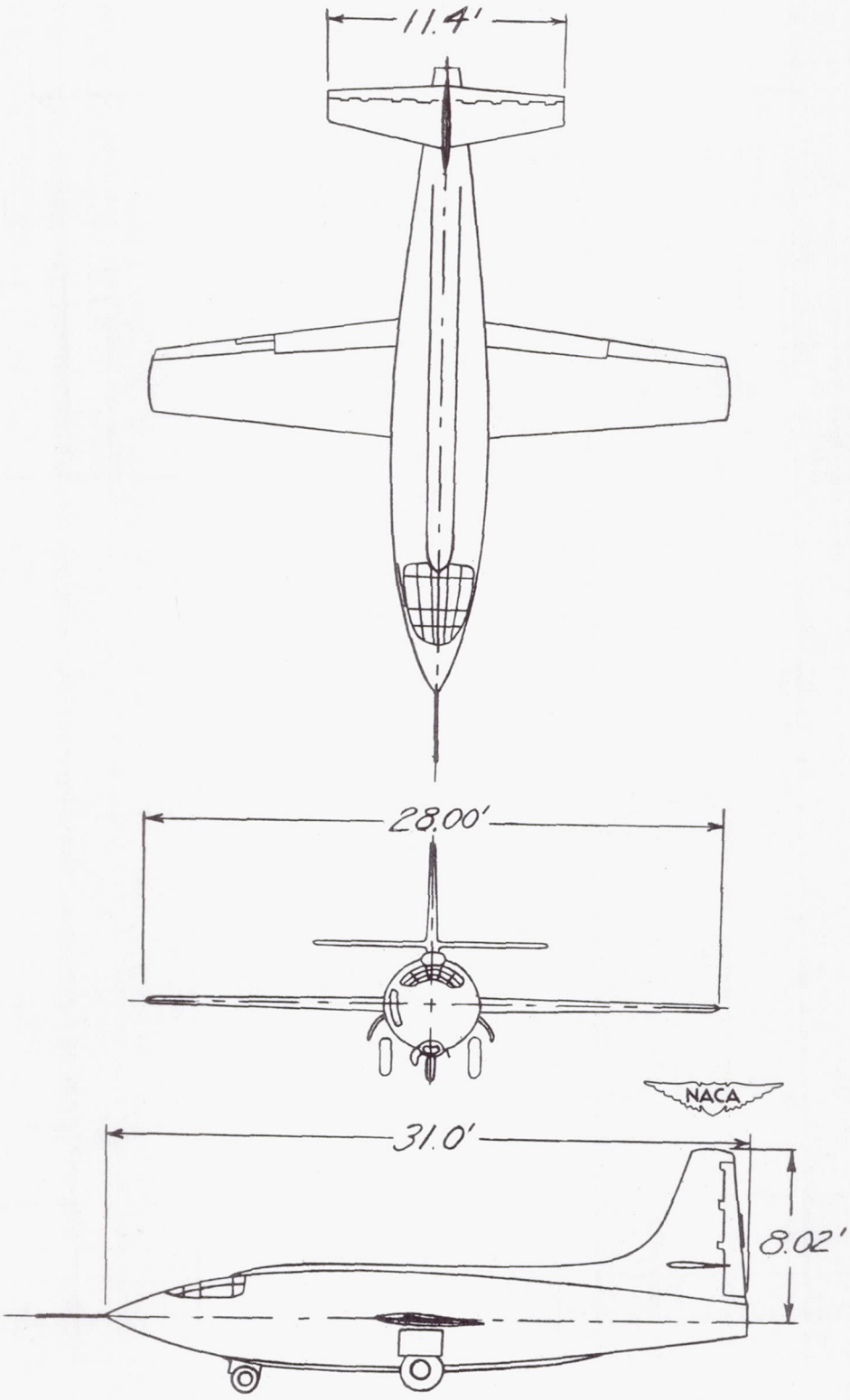

Figure 2.- Three-view drawing of Bell X-1 airplane.

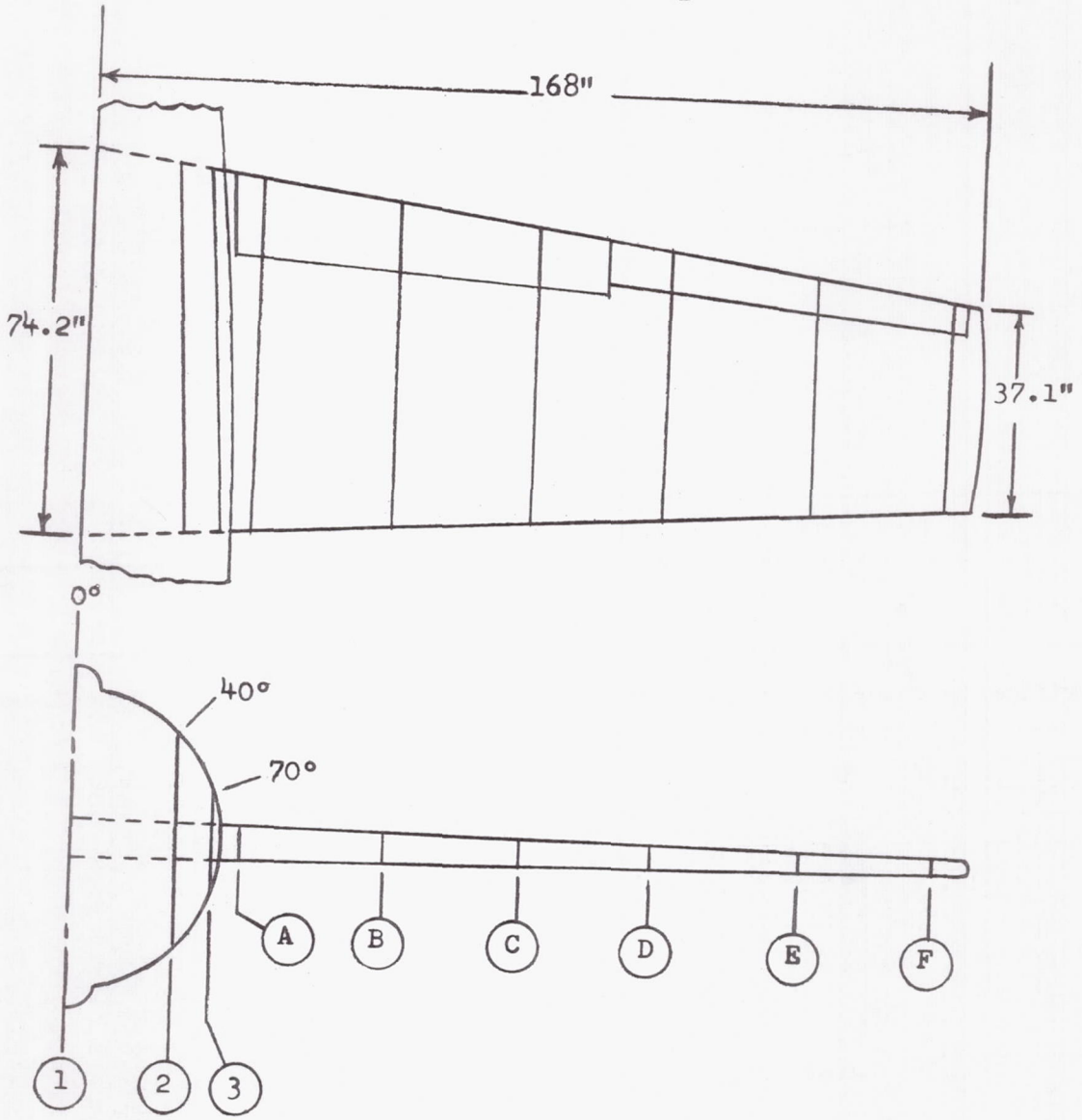

Spanwise station	1	2	3	A	B	C	D	E	F
Distance from airplane center line, percent b/2	0	10.7	14.9	18.4	33.8	49.1	64.4	79.8	95.1

(a) Spanwise locations.

Figure 3.- Spanwise and chordwise locations of pressure measuring orifices.

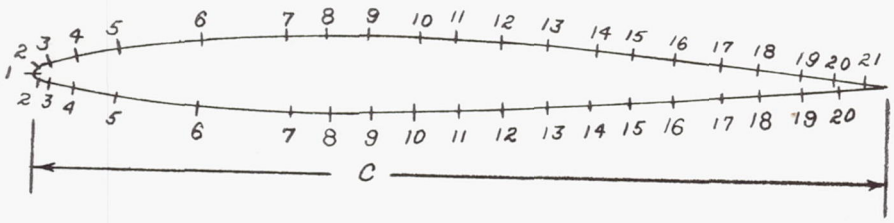

Orifice station location, percent chord												
Span Station	A		B		C		D		E		F	
Orifice	Upper	Lower	Upper	Lower	Upper	Lower	Upper	Lower	Upper	Lower	Upper	Lower
1	0		0		0		0		0		0	
2	1.16	1.16	1.43	1.26	1.18	1.28	1.29	1.38	1.17	1.17	1.16	1.23
3	2.40	2.40	2.72	2.59	2.40	2.40	2.66	2.66	2.27	2.27	2.64	2.39
4	4.79	4.79	5.21	5.06	5.04	5.04	5.16	5.16	4.90	4.90	5.49	5.03
5	9.85	9.98	10.45	10.45	9.64	9.64	10.95	10.95	8.91	8.91	10.42	10.16
6	19.75	19.92	20.00	20.00	20.00	20.00	19.76	20.10	20.00	19.90	19.92	19.66
7	29.80	30.00	29.40	30.00	29.32	30.00	30.00	30.00	30.00	30.00	29.75	29.62
8	34.85	35.05	34.45	35.20	34.78	35.20	34.80	35.10	35.00	34.92	35.05	35.05
9	40.00	40.10	39.90	40.00	39.58	40.00	40.00	40.15	40.00	40.00	40.07	40.07
10	45.10	45.00	45.17	45.38	44.40	45.92	45.15	45.35	45.15	44.52	45.00	45.00
11	50.20	49.70	50.10	49.95	49.52	50.18	50.18	50.30	50.08	49.90	50.02	50.00
12	54.90	54.90	55.00	54.92	55.10	55.20	55.28	55.28	55.50	54.90	55.05	54.95
13	60.38	60.00	61.08	59.82	59.90	60.00	60.80	60.60	59.50	60.50	59.70	60.00
14	65.00	65.00	65.20	65.00	65.00	65.00	65.40	65.60	64.95	65.00	64.95	64.95
15	70.00	70.00	70.15	70.15	70.00	70.00	69.85	69.95	69.90	70.00	70.05	70.05
16	74.10	74.42	74.00	74.00	74.00	74.38	74.40	74.20	73.70	74.60	73.85	74.30
17	78.60	78.60	78.60	78.60	78.00	78.20	79.50	79.70	81.00	80.50	79.85	80.05
18	84.90	85.08	85.10	85.00	84.95	84.95	85.62	85.40	85.70	85.70	85.70	85.70
19	90.00	90.00	90.30	89.96	90.00	90.00	90.00	90.00	89.95	89.95	89.60	89.60
20	94.80	94.80	95.00	94.50	95.00	95.10	95.00	95.00	95.00	95.30	95.10	95.30
21	97.65	—	97.60	—	97.30	—	97.10	—	96.70	—	96.10	—

NACA

(b) Chordwise locations; wing stations.

Figure 3.- Continued.

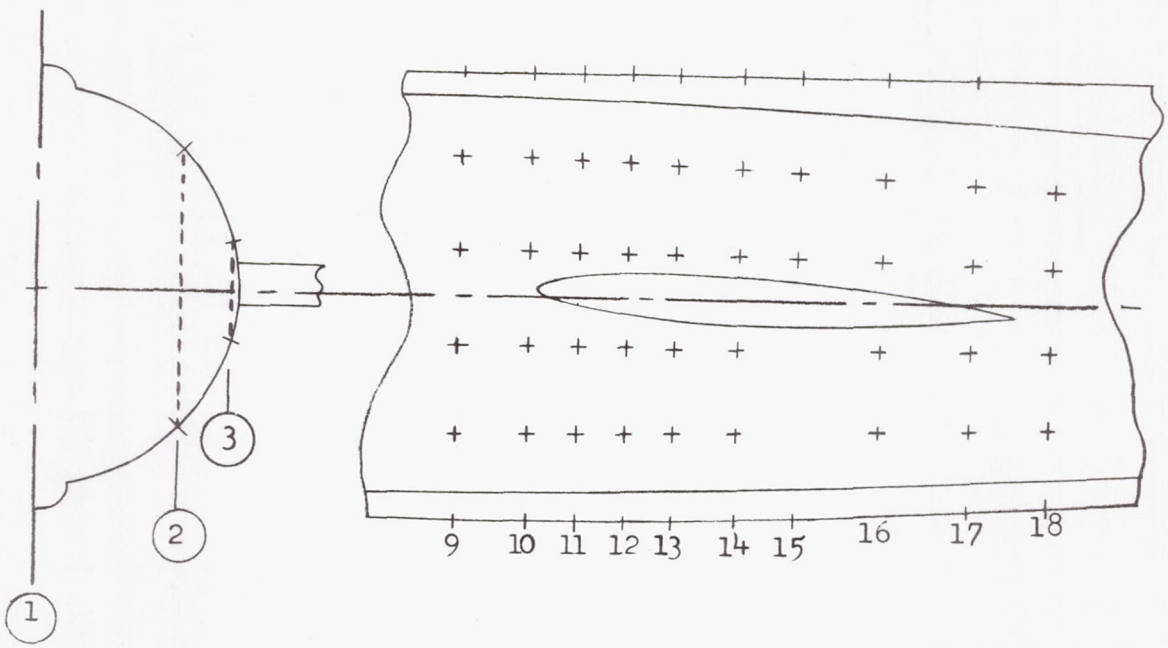

	Orifice station location, percent chord					
	Row 1		Row 2		Row 3	
Orifice	Upper	Lower	Upper	Lower	Upper	Lower
9	-10.9	-11.1	-13.8	-14.0	-15.0	-15.2
10	2.6	4.9	0.4	3.6	-0.4	2.1
11	10.6	13.8	9.0	11.7	8.3	10.1
12	21.4	23.1	20.4	20.6	20.0	20.4
13	30.9	30.9	30.4	30.4	30.1	30.1
14	43.0	43.0	43.2	43.2	43.3	43.3
15	53.8	54.7	54.6	--	54.9	--
16	71.4	--	73.1	74.0	73.9	77.0
17	86.8	87.3	89.5	89.5	90.6	90.6
18	--	103.0	107.0	106.5	108.0	108.0

NACA

(c) Chordwise locations; fuselage stations.

Figure 3.- Concluded.

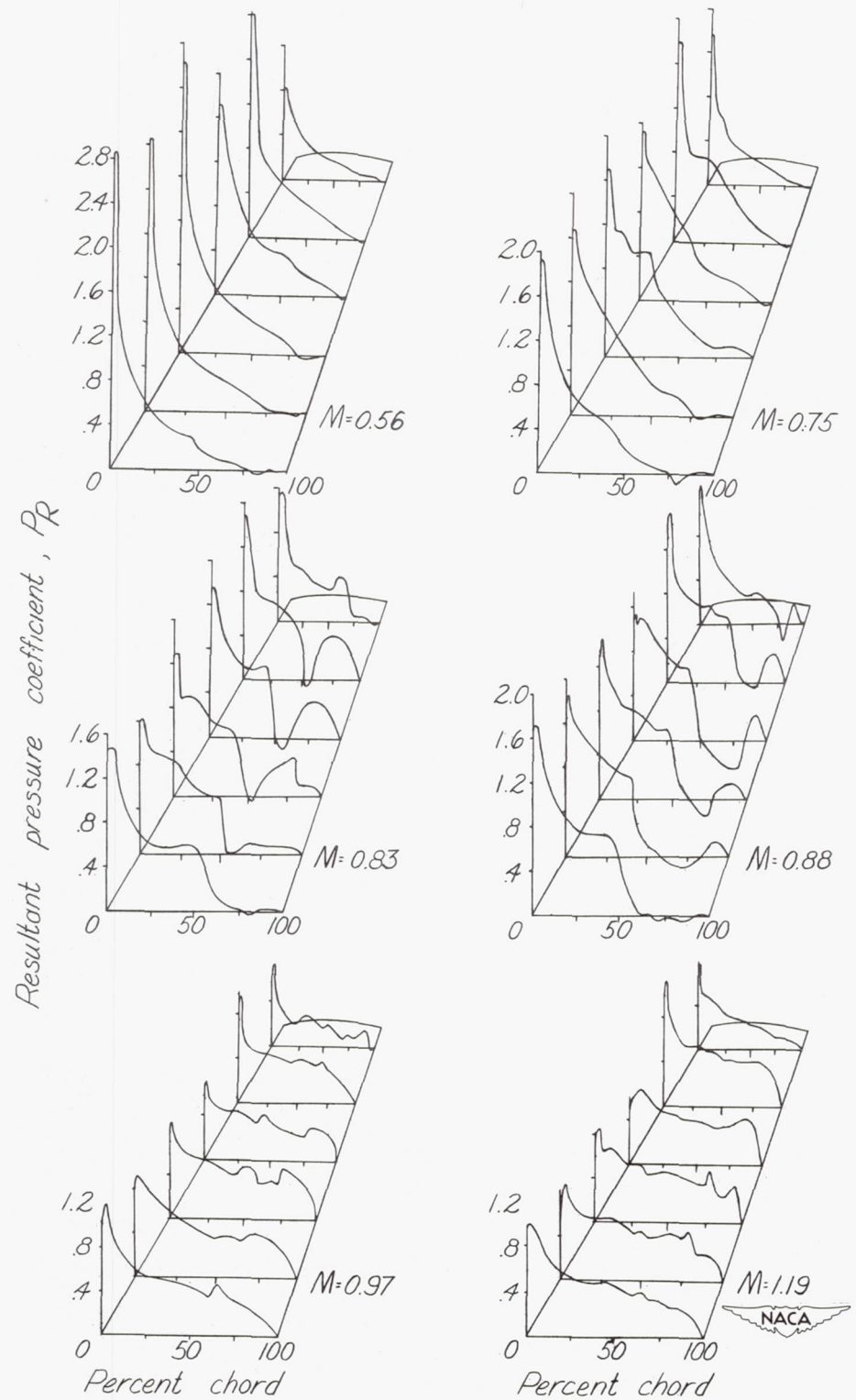

Figure 4.- Isometric views of load distribution on the wing panel of the Bell X-1 airplane at various Mach numbers. C_{N_P} = 0.3.

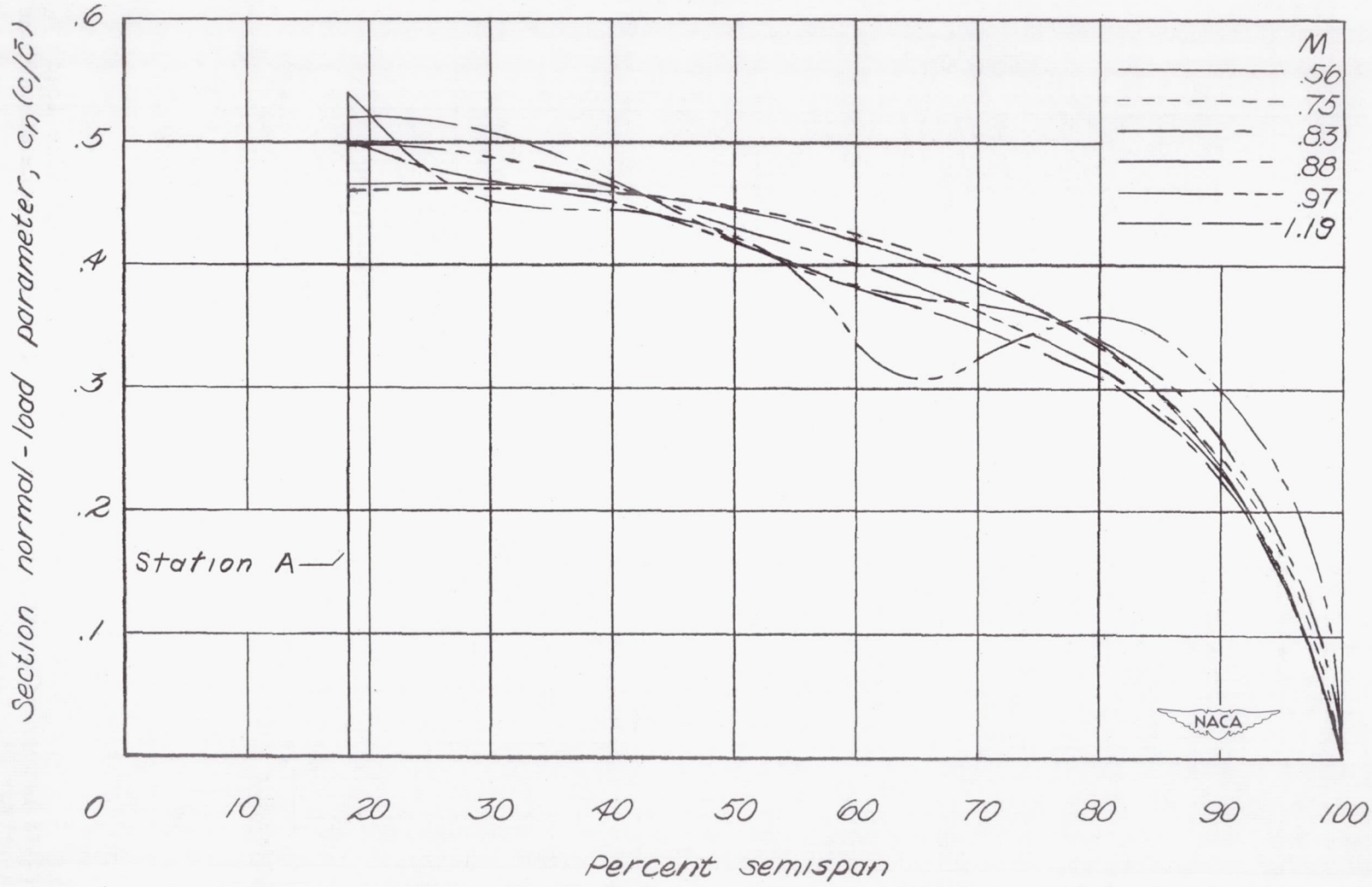

Figure 5.- Spanwise load distributions on the wing panel of the Bell X-1 airplane at various Mach numbers. $C_{N_P} = 0.3$.

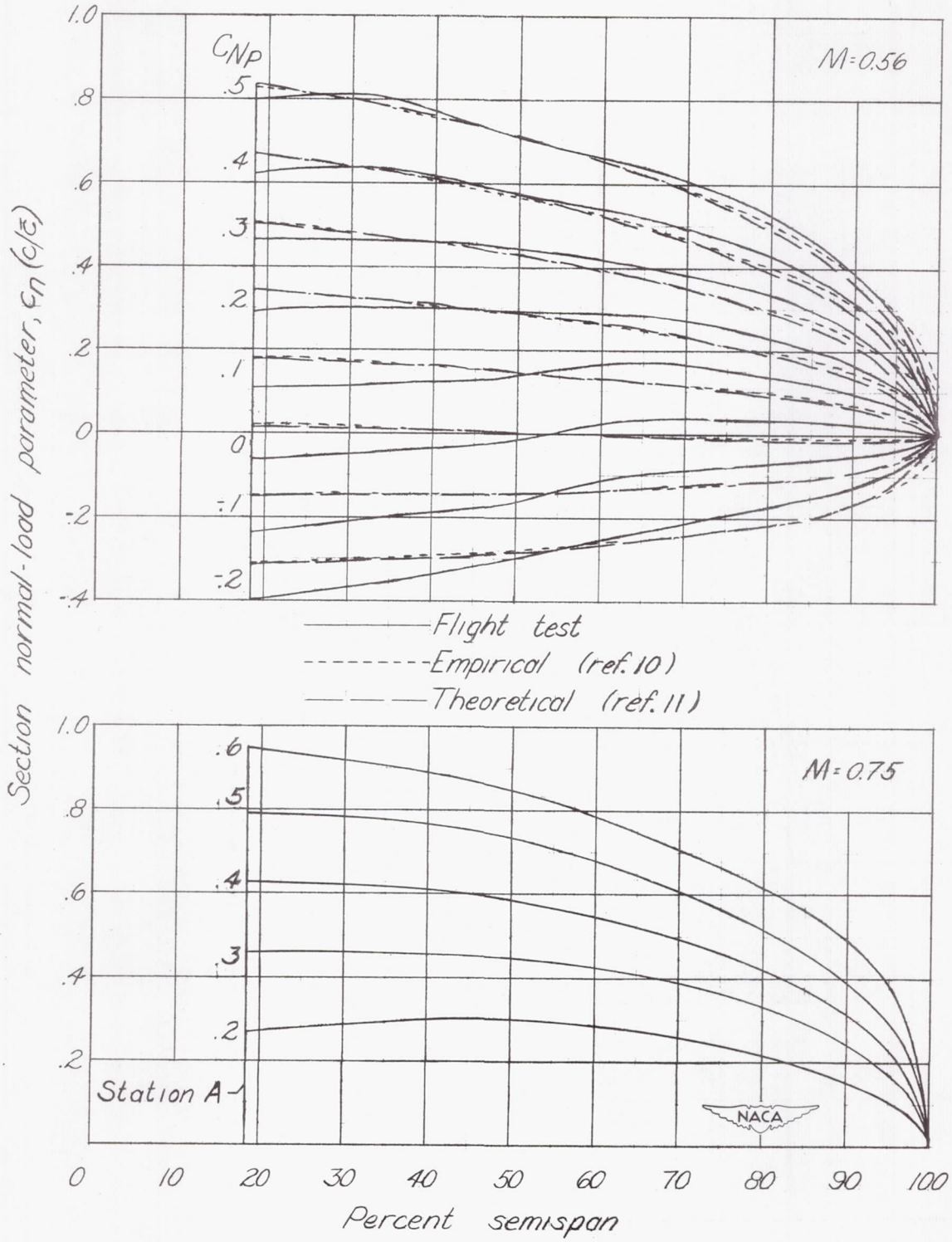

Figure 6.- Effects of normal-force coefficient on the spanwise load distribution over the wing panel of the Bell X-1 airplane at various Mach numbers.

NACA-Langley - 11-23-53 - 350

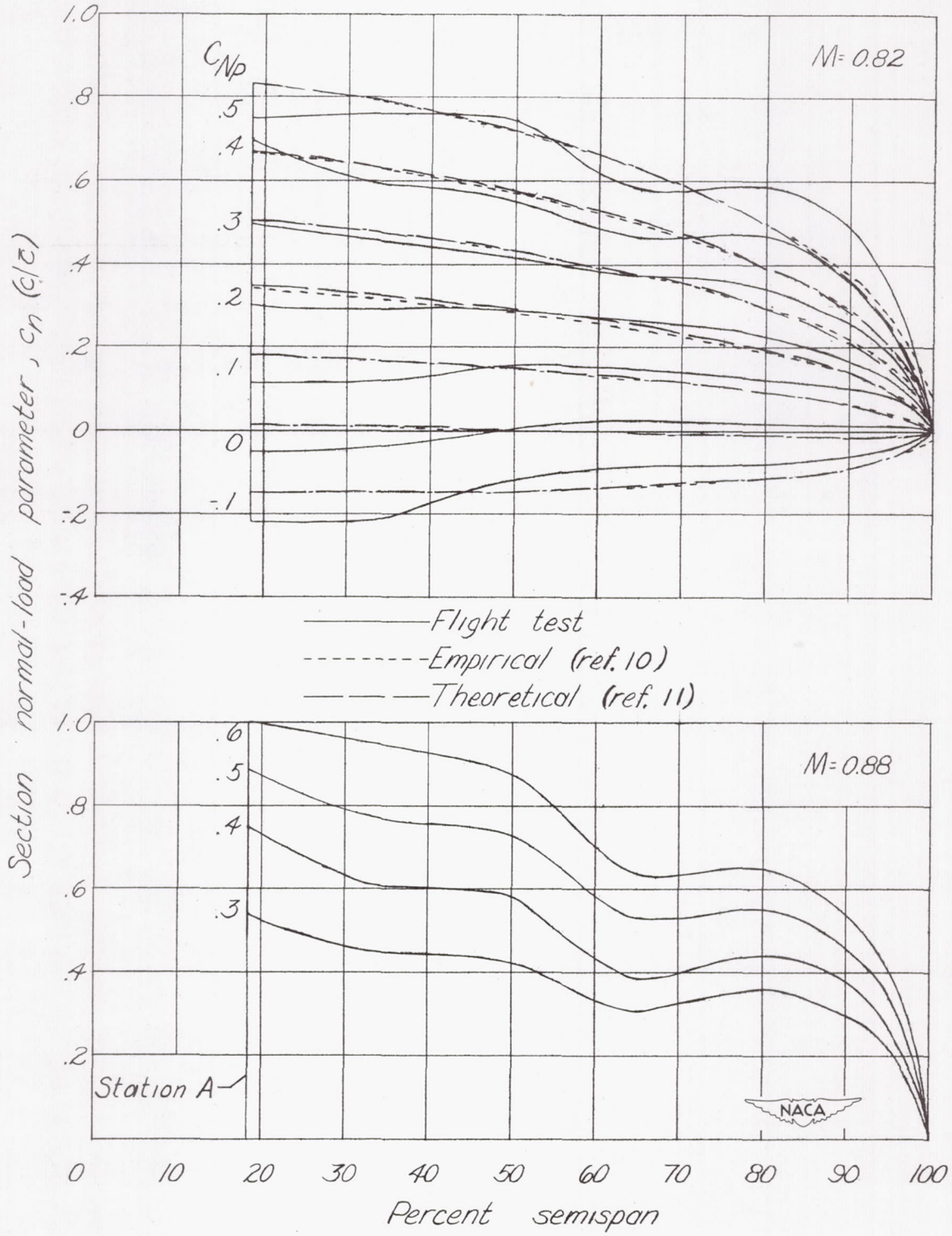

Figure 6.- Continued.

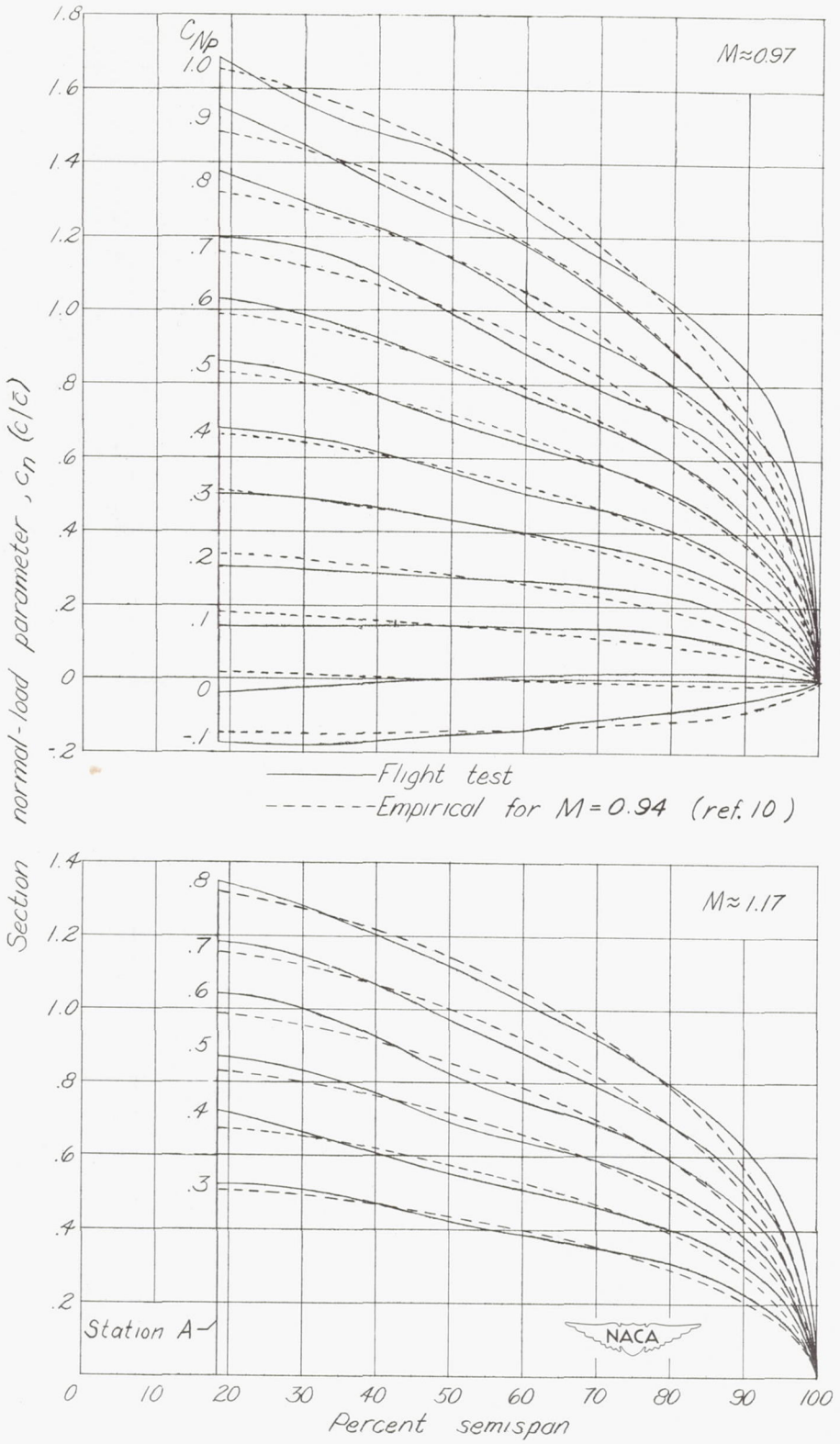

Figure 6.- Concluded.

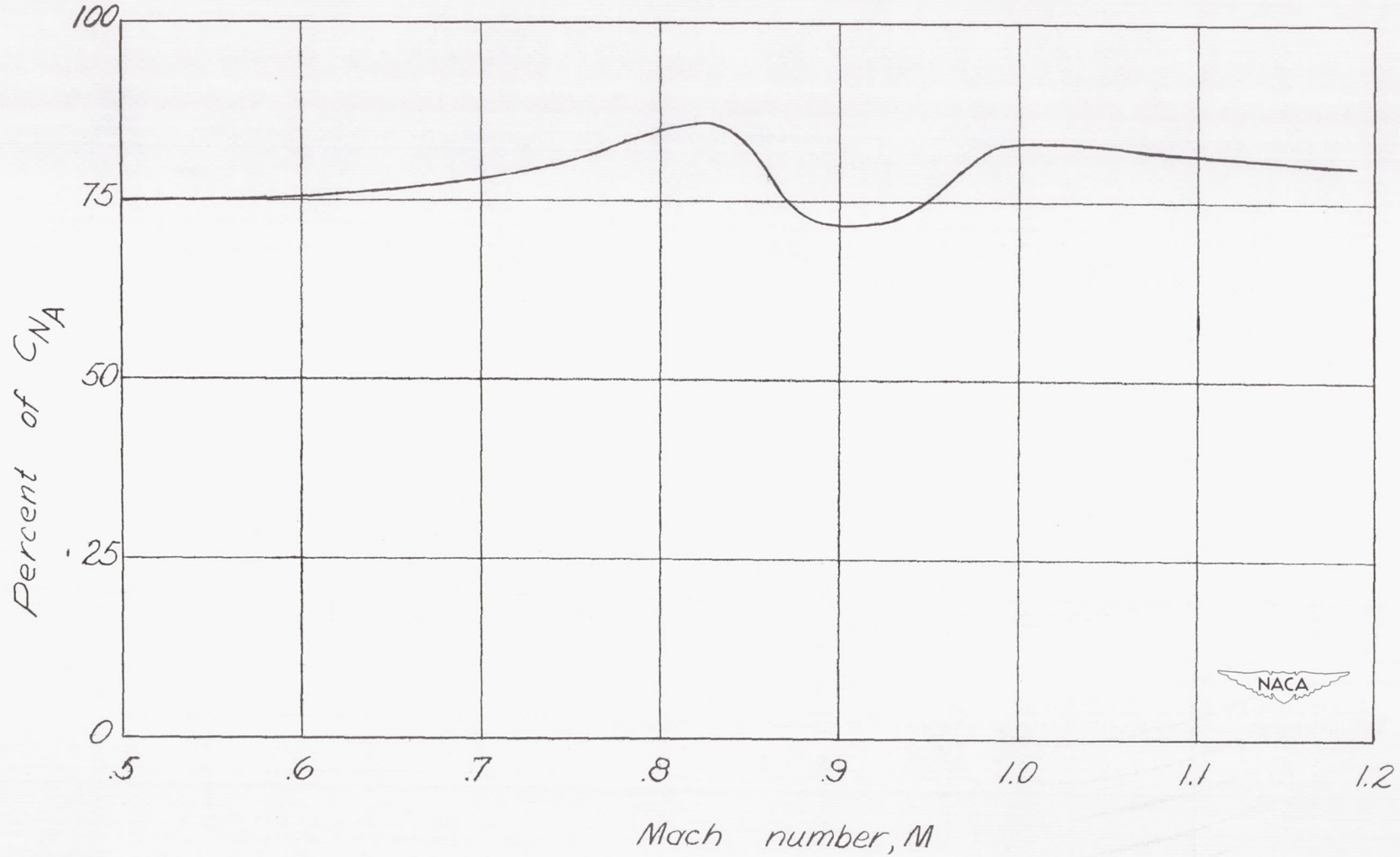

Figure 7.- Approximate portion of the airplane normal-force coefficient carried by the wing panels. C_{N_A} = 0.3 to 0.7.

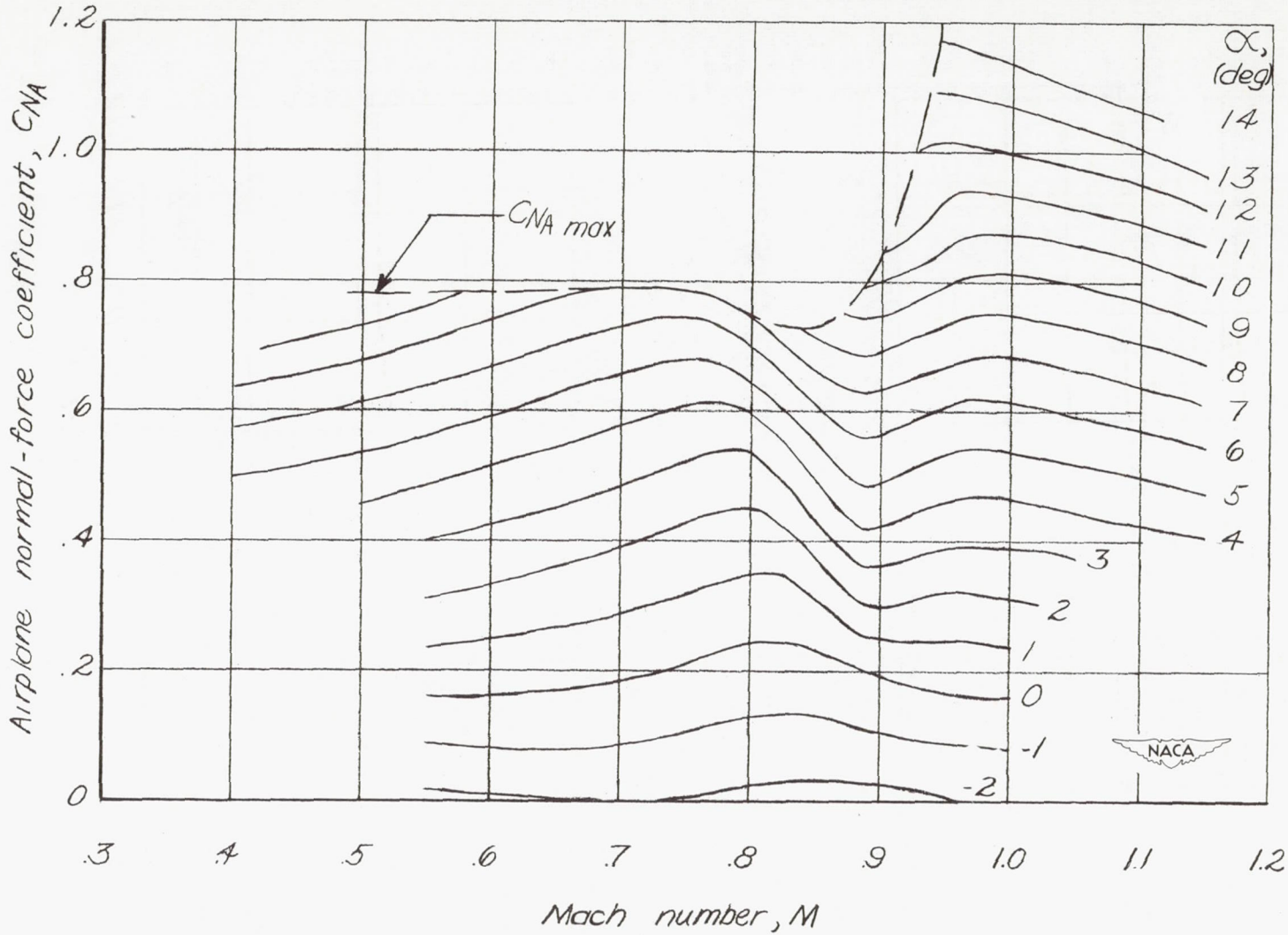

Figure 8.- Approximate variation of airplane normal-force coefficient with Mach number for various angles of attack.

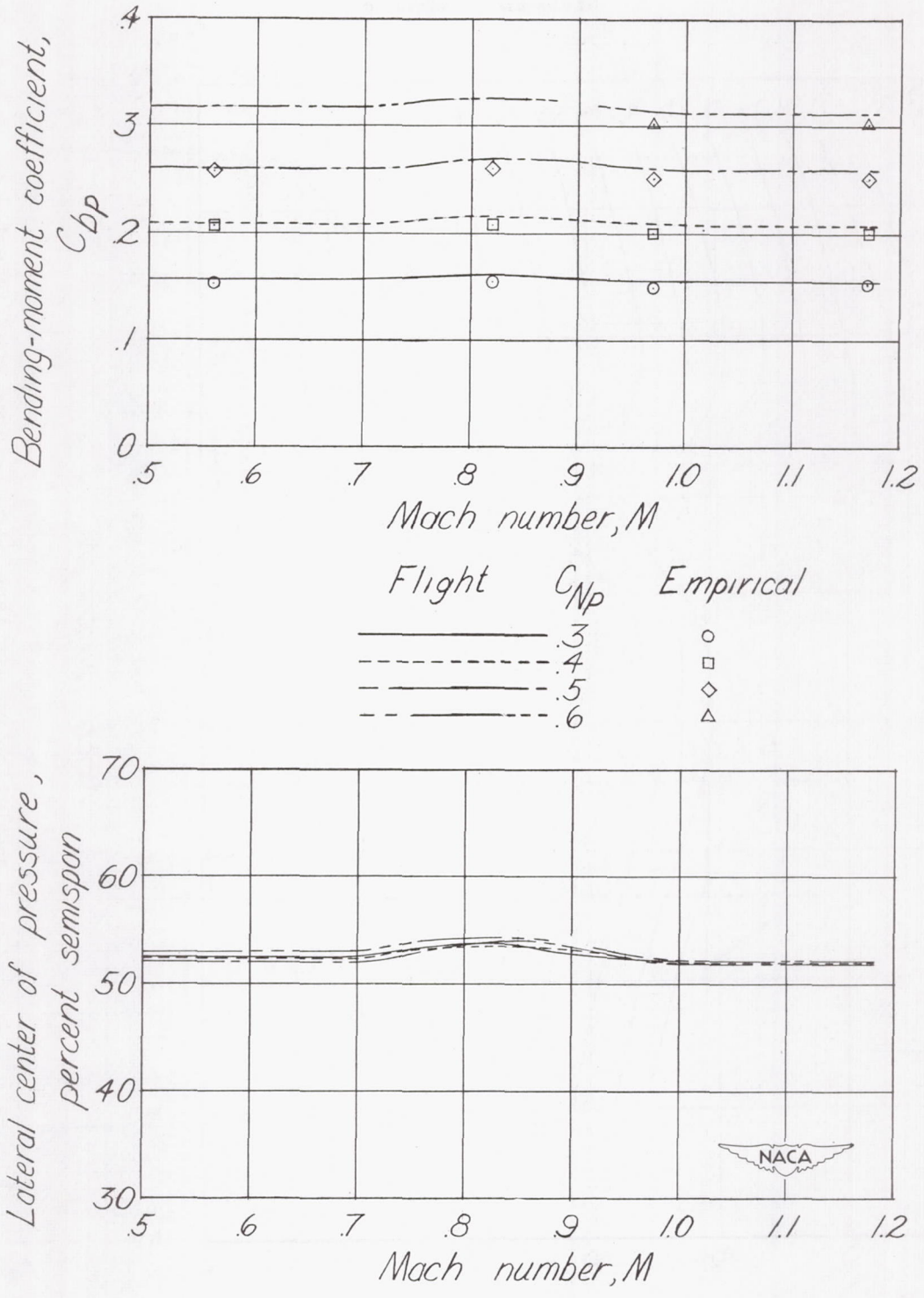

Figure 9.- Variation with Mach number of the lateral center of pressure and bending-moment coefficient for the wing panel of the Bell X-1 airplane.

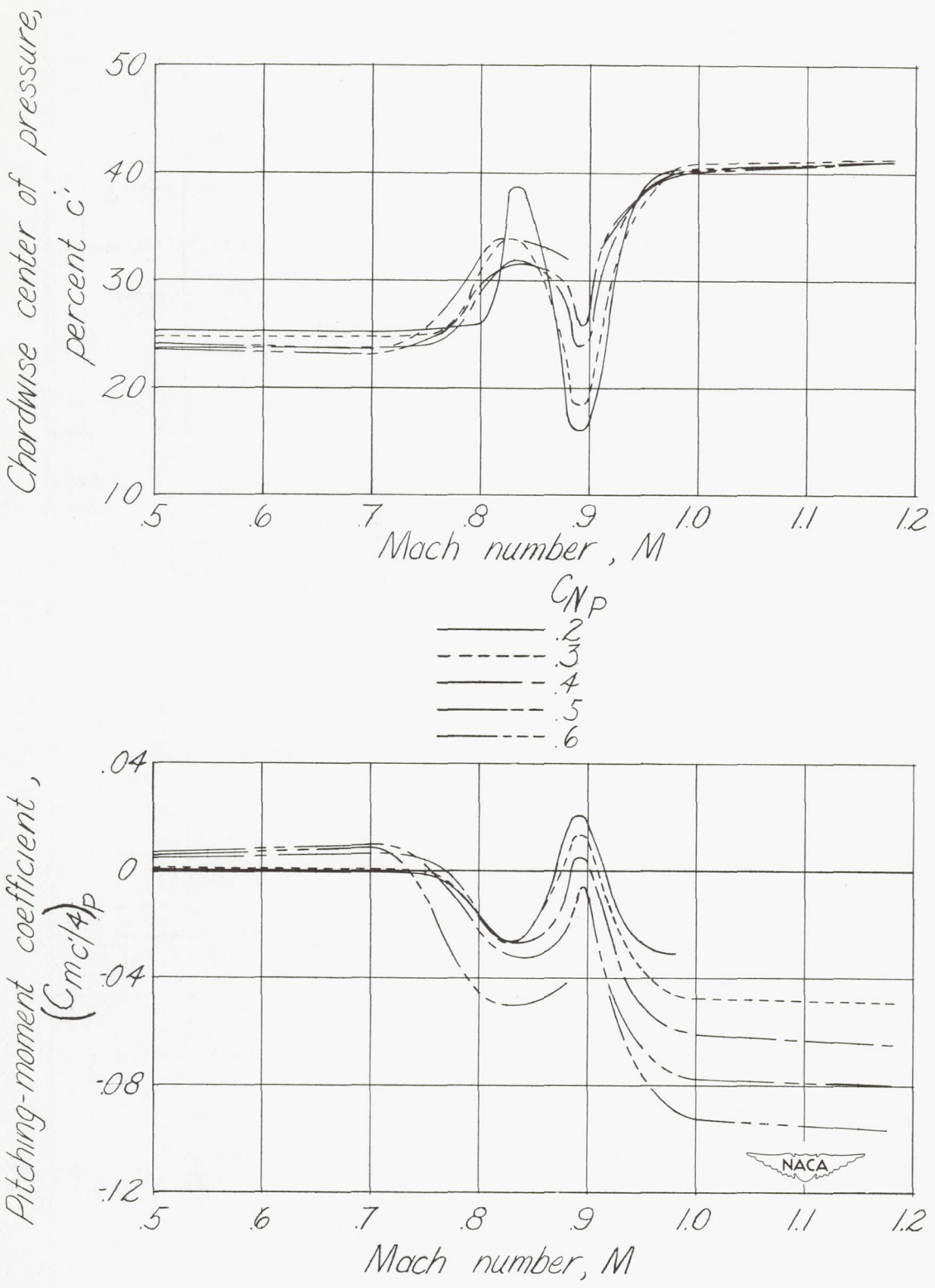

Figure 10.- Variation with Mach number of the chordwise center of pressure and pitching-moment coefficient for the wing panel of the Bell X-1 airplane.

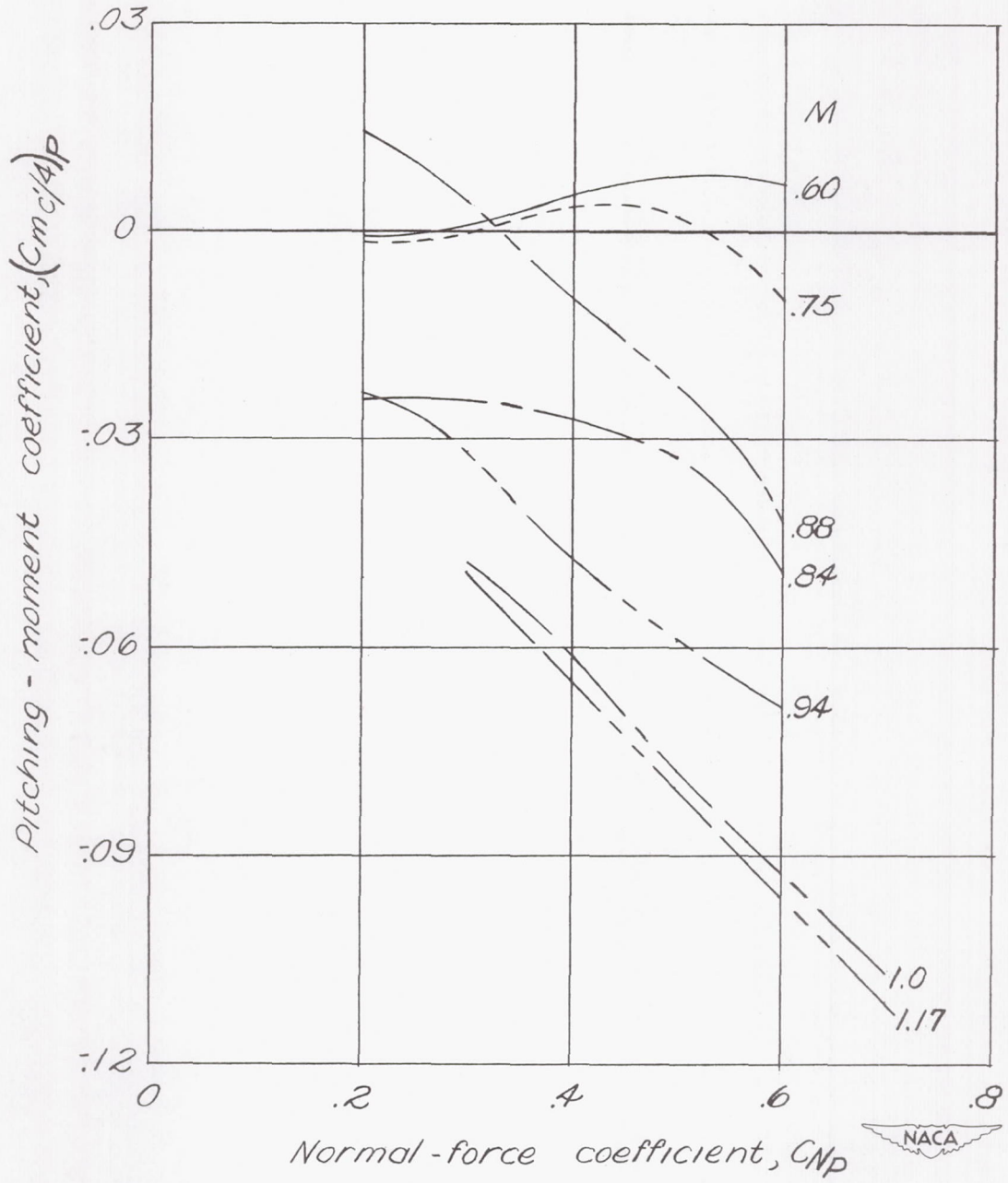

Figure 11.- Variation of pitching-moment coefficient with normal-force coefficient for the wing panel of the Bell X-1 airplane at various Mach numbers.

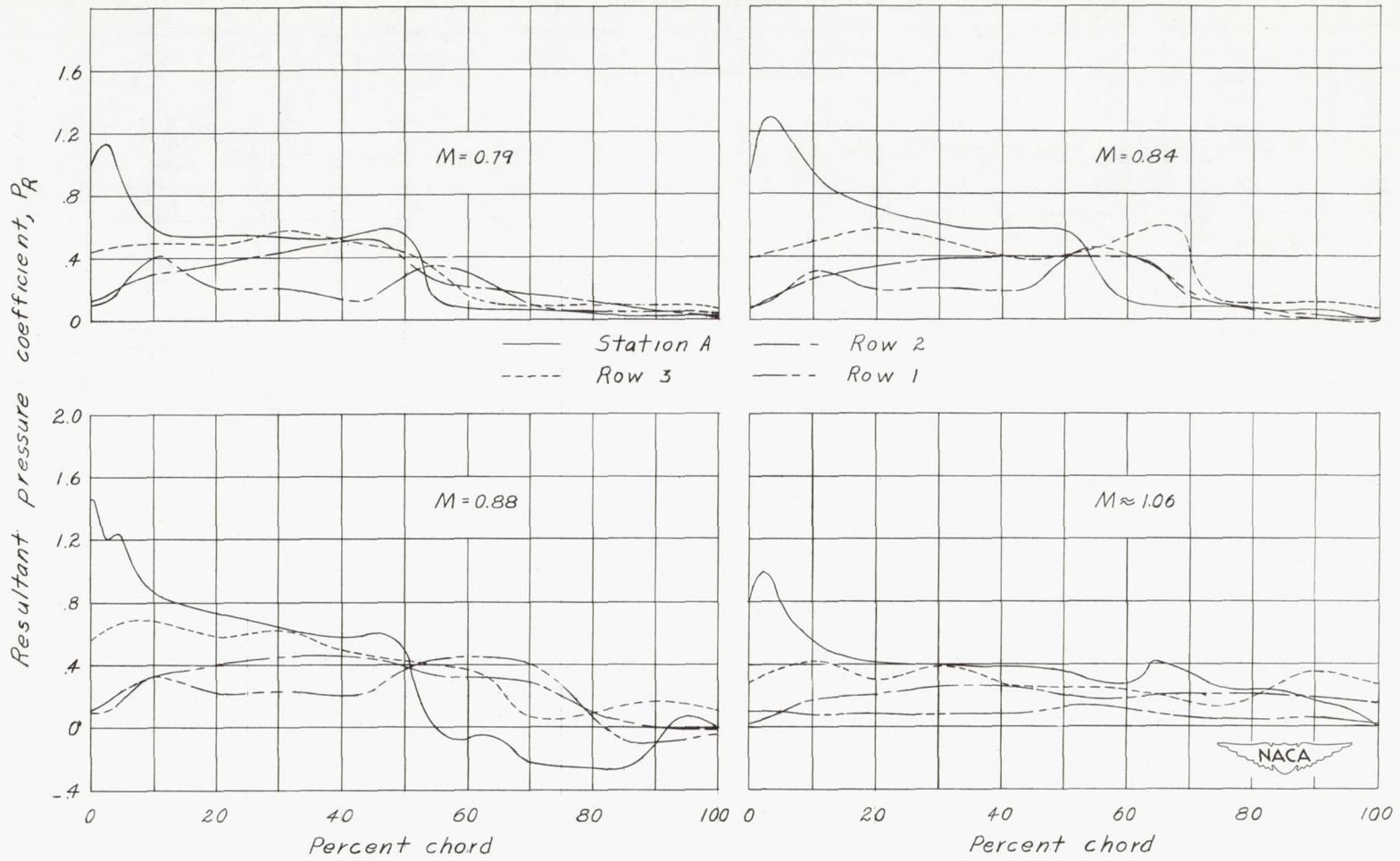

(a) $C_{N_A} = 0.35$.

Figure 12.- Comparison of the chordwise load distributions on the fuselage stations with that of wing station A at selected Mach numbers.

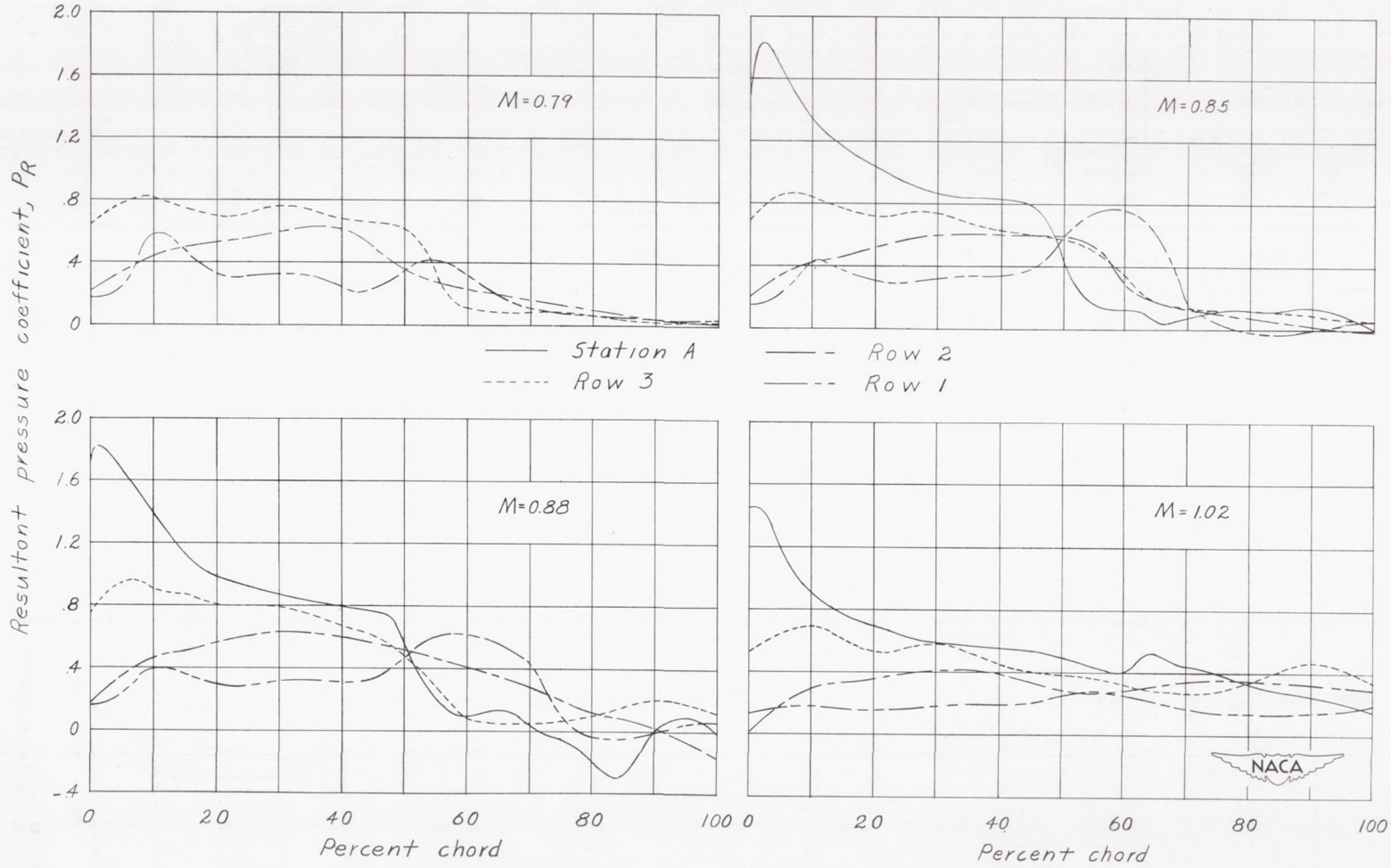

(b) $C_{N_A} = 0.50$.

Figure 12.- Continued.

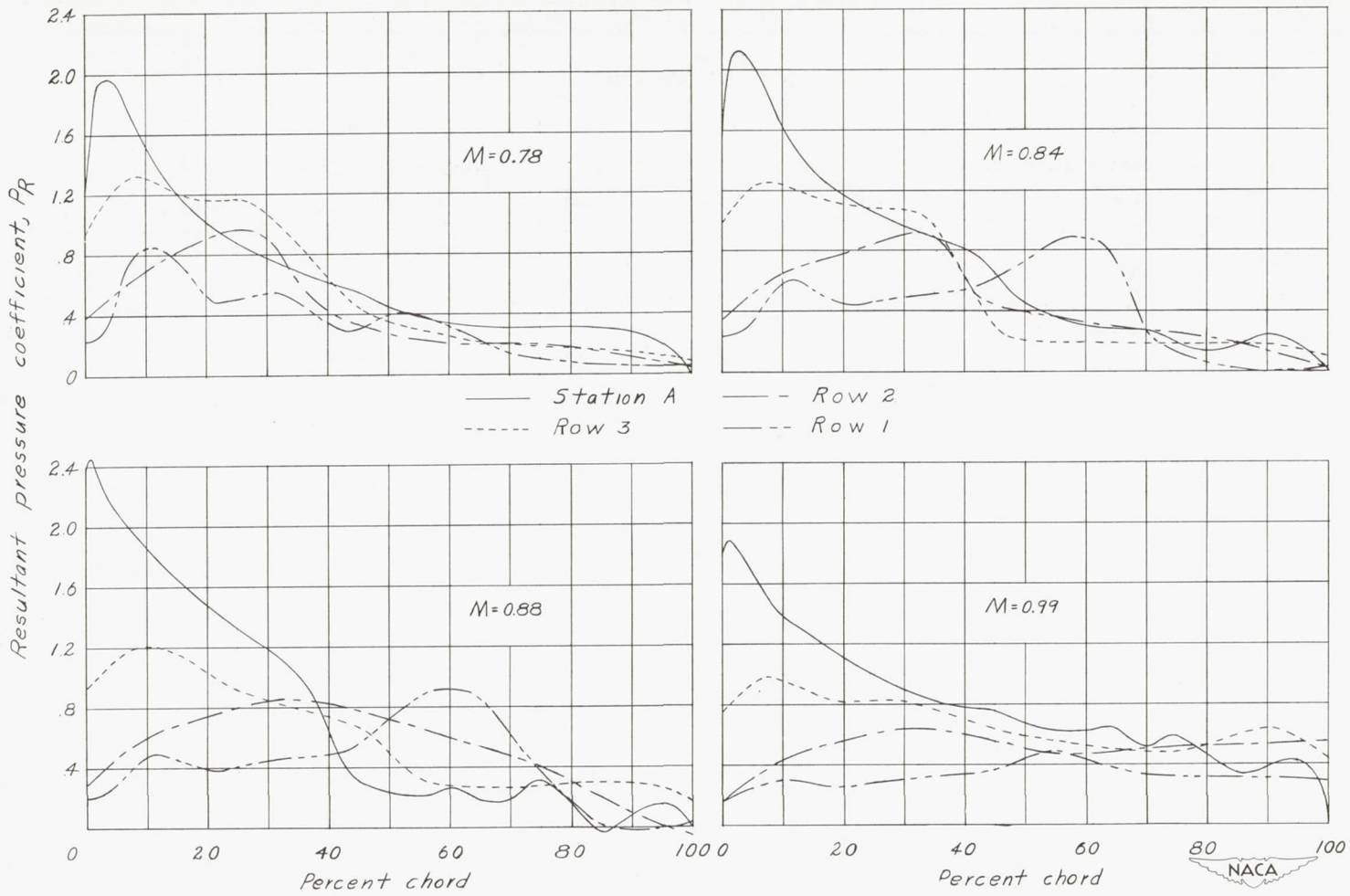

(c) $C_{N_A} = 0.70$.

Figure 12.- Concluded.

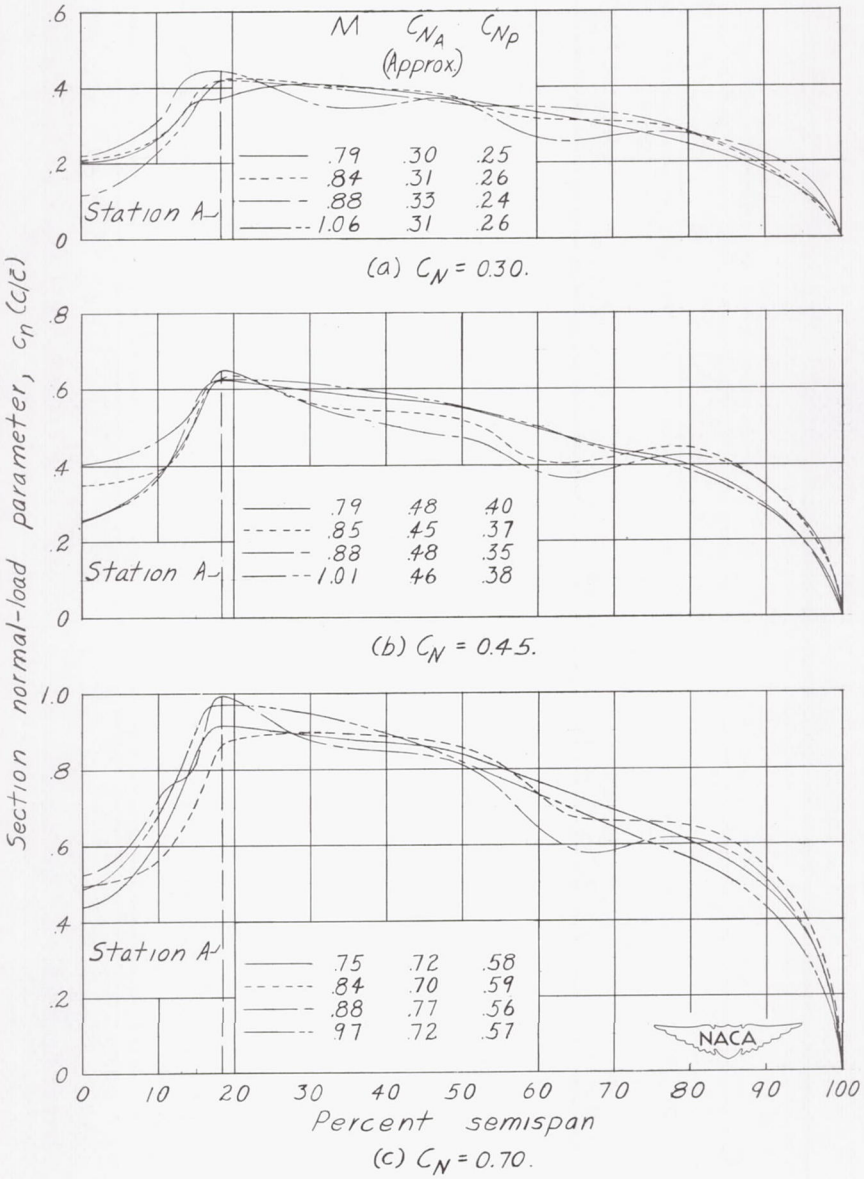

Figure 13.- Effects of Mach number on spanwise load distribution (including wing to fuselage carry over) at various normal-force coefficients.

NACA-Langley - 11-4-53 - 325

CONFIDENTIAL